ON SUBHARMONIC AND FUNDAMENTAL INSTABILITY MODES IN BOUNDARY LAYERS

Márcio T. Mendonça
Centro Técnico Aeroespacial - Instituto de Atividades Espaciais
Pç Mal. Eduardo Gomes, 50 - 12228-904 - São José dos Campos - SP - Brazil
email: marcio_tm@yahoo.com
Marcello A. F. de Medeiros
Pontifícia Universidade Católica de Minas Gerais - Engenharia Mecânica
Av. Dom José Gaspar, 500 - 30535-610 - Belo Horizonte - MG - Brazil
email: marcello@pucminas.br

Summary. *In this paper a numerical model based on the parabolized stability equations is used to investigate the characteristics of subharmonic and fundamental secondary instabilities. In order to identify which instability mode is dominant, the classic K-type and H-type secondary instability experiments are repeated including both fundamental and subharmonic oblique modes in the initial condition. The results show that, depending on the initial amplitude of the two-dimensional Tollmien-Schlichting (TS) wave, both oblique modes are destabilized and that the subharmonic oblique wave has a stronger nonlinear growth. Linearly unstable oblique modes are also studied showing that, due to its higher frequency, the fundamental mode grows faster and interact more strongly with the two-dimensional TS wave. Which secondary instability mode will prevailes depends on the relative amplitude of the disturbances and on their growth rates.*

Keyword: *hydrodynamic instability, transition to turbulence, K-type secondary instability, H-type secondary instability, Tollmien-Schlichting waves.*

1. INTRODUCTION

After an initial stable laminar flow downstream of the leading edge, the boundary layer becames unstable for infinitesimal disturbances of certain frequencies. The first unstable disturbances are two-dimensional (2D) waves that travel in the mean flow direction. They are known as Tollmien-Schlichting waves. Due to random noise in the flow field, three-dimensional (3D) disturbances are also present and propagate in a direction oblique to the mean flow direction. The nonlinear interaction between plane waves and small amplitude oblique waves often generates a spanwise periodic variation that develop into Lambda shaped structures which, in turn form either an aligned row pattern or an staggered row

pattern. Which row pattern will appear depends on the relative frequency of the 2D and 3D interacting waves. Kachanov and Levchenko (1984) identified that for 3D waves with half the frequency of the 2D waves the Lambda shaped structures are staggered by half spanwise wavelength. For 3D and 2D waves with the same frequency the Lambda shaped structures are aligned. This second breakdown process was identified by Klebanoff, Tidstrom and Sargent (1962). These flow patterns are called subharmonic (H-type) secondary instability and fundamental (K-type) secondary instability respectively. They result in the evolution of spanwise variations of the streamwise velocity profile forming peak and valley regions and generate vortices that in a smoke wire visualization experiment would concentrate smoke in certain regions forming the Lambda shapes. At the peak of the Lambda structures the local vorticity is high and the structures breakdown in bursts of turbulent spots which appear randomly in the flow field. Further downstream, these turbulent spots coalesce into a fully developed turbulent boundary layer. Herbert used secondary stability theory to study fundamental and subharmonic secondary instability and was able to reproduce the characteristic lambda structure observed experimentally. He presented a review of secondary instability theory along with details on the different instability modes observed experimentally and numerically (1988).

Given that the natural disturbances in a given flow field are composed of random noise, only in controlled experiments it is possible to force either K-type or H-type secondary instability. In natural conditions it is more likely that both K-type and H-type secondary instabilities will compete or interact, modifying the pattern of the Lambda shaped structure. The present work investigate the nonlinear development of disturbances composed of a 2D Tollmien-Schlichting wave with frequency 'f', a pair of 3D waves with frequency '$1/2f$', and a pair of 3D waves with frequency 'f'. The results show that, by changing the relative amplitude of the different disturbances it is possible to select the resonant mechanism that dominates.

In the paper, the results obtained by Kachanov and Levchenko for H-type secondary instability and by Klebanoff, Tidstrom and Sargent for K-type secondary instability are reproduced with a numerical model base on the Parabolized Stability Equations. The same model is then used to conduct the numerical experiments described above for different values of disturbance initial amplitudes and spanwise wavenumber. Results for the growth of different harmonics are presented showing whether K-type or H-type secondary instability prevails. The vorticity distributions are also presented.

2. FORMULATION

Details of the derivation of the Parabolized Stability Equations (PSE) and of the numerical procedure used in the present investigation have been presented elsewhere (Mendonça *et al.* , 2000b; Mendonça *et al.* , 2000a). In this section only the main points are presented.

The Navier-Stokes equations for an incompressible flow of a Newtonian fluid are simplified by assuming that the dependent variables are decomposed into a mean component and a fluctuating component as follows:

$$\vec{u^*} = \vec{U^*} + \vec{u'^*}, \qquad \text{and} \qquad p^* = P^* + p'^*, \tag{1}$$

where $\vec{u^*} = [u^*, v^*, w^*]^T$ is the velocity vector and p^* is the pressure. The superscript '$*$' indicates dimensional variables. The coordinate system is based on the streamlines (ψ^*) and potential lines (ϕ^*) of the inviscid flow.

The equations are nondimensionalized using δ_0^* and U_∞^* as the length and velocity scaling parameters. $\delta_0^* = (\nu^* \phi_0^* / U_\infty^*)^{1/2}$ is the boundary layer thickness parameter, U_∞^* is the free stream velocity, ϕ_0^* is a reference length taken as the streamwise location where initial conditions are applied, and ν^* is the kinematic viscosity. The Reynolds number is defined as: $Re = U_\infty^* \delta_0^* / \nu^*$.

The mean flow is governed by Prandtl boundary layer equations for the flow over a flat plate. The perturbation Φ' is assumed to be composed of a slowly varying shape function and an exponential oscillatory wave term. It is represented mathematically as a double Fourier expansion truncated to a finite number of modes:

$$\Phi' = \sum_{n=-N}^{N} \sum_{m=-M}^{M} \Phi_{n,m}(\phi, \psi) \exp\left[\int_{\phi_0}^{\phi} a_{n,m}(\xi) d\xi + im\beta z - in\omega t \right], \tag{2}$$

$$a_{n,m}(\phi) = \gamma_{n,m}(\phi) + in\alpha(\phi). \tag{3}$$

where $\Phi_{n,m}(\phi, \psi) = [u_{n,m}, v_{n,m}, w_{n,m}, p_{n,m}]^T$ is the complex shape function vector. This procedure is similar to a normal mode analysis, but, in this case, the shape function $\Phi_{n,m}$ is a function of both ϕ and ψ.

The streamwise growth rate $\gamma_{n,m}$, the streamwise wavenumber α, and the spanwise wavenumber β were nondimensionalized using the boundary layer thickness parameter δ_0^*. The frequency ω was nondimensionalized using the free stream velocity U_∞^* and the boundary layer thickness parameter δ_0^* .

The perturbation variable Φ', as defined in Eq. (2), is substituted in the governing equations. By assuming that the shape function, wavelength, and growth rate vary slowly in the streamwise direction, second order derivatives and products of first order derivatives with respect to the streamwise coordinate can, therefore, be neglected. After performing a harmonic balance in the frequency, a set of coupled nonlinear equations is obtained. These resulting equations are known as the Parabolized Stability Equations (PSE). For each mode (n, m) an equation in vector form results:

$$\overline{A}_{n,m}\Phi_{n,m} + \overline{B}_{n,m}\frac{\partial \Phi_{n,m}}{\partial \phi} + \overline{C}_{n,m}\frac{\partial \Phi_{n,m}}{\partial \psi} + \overline{D}_{n,m}\frac{\partial^2 \Phi_{n,m}}{\partial \psi^2} = \frac{\overline{E}_{n,m}}{e^{\int_{\phi_0}^{\phi} a_{n,m}(\xi) d\xi}}, \tag{4}$$

where the coefficient matrices can be found in Mendonça (1997).

The resulting equations are parabolic in ϕ and the solution can be marched downstream given initial conditions at a starting position ϕ_0. The approach is correct as long as the instabilities are convective and propagate in the direction of the mean flow without affecting the flow field upstream.

The boundary conditions for Eq. (4) are given by homogeneous Dirichlet no-slip conditions at the wall, Neumann boundary conditions for the velocity components in the far field, and homogeneous Dirichlet condition for pressure in the far field. Initial conditions at a starting position ϕ_0 downstream of the leading edge are obtained from Orr-Sommerfeld solutions for Tollmien-Schlichting waves.

2.1 Normalization condition

The splitting of the perturbation $\Phi'(\phi, \psi, z, t)$ in Eq. (2) into two functions, $\Phi_{n,m}(\phi, \psi)$ and $a_{n,m}(\phi)$, is ambiguous, since both are functions of the streamwise coordinate ϕ. It is

necessary to define how much of the variation will be represented by the shape function $\Phi_{n,m}(\phi,\psi)$, and how much will be represented by the complex wavenumber $a_{n,m}(\phi)$. This definition has to guarantee that rapid changes in the streamwise direction are avoided so that the hypothesis of slowly changing variables is not violated. Fast variations of the shape function $\Phi_{n,m}(\phi,\psi)$ in the streamwise direction are transfered to the streamwise complex wavenumber $a_{n,m}(\phi) = \gamma_{n,m}(\phi) + in\alpha(\phi)$. If this variation is represented by $b_{n,m}$, for each step in the streamwise direction it is necessary to iterate on $a_{n,m}(\phi)$ until $b_{n,m}$ is smaller than a given threshold. At each iteration k, $a_{n,m}(\phi)$ is updated according to $(a_{n,m})_{k+1} = (a_{n,m})_k + (b_{n,m})_k$.

The variation $b_{n,m}$ of the shape function can be monitored in different ways. Possible choices are presented below.

$$b_{n,m} = \frac{1}{\int_0^\infty ||\vec{u}_{n,m}||^2 d\psi} \int_0^\infty \left(\vec{u}^{\dagger}_{n,m} \cdot \frac{\partial \vec{u}_{n,m}}{\partial \phi} \right) d\psi, \tag{5}$$

In Eq. 5 $\vec{u}^{\dagger}_{n,m}$ is the complex conjugate of $\vec{u}_{n,m}$. The integral of $||\vec{u}_{n,m}||^2$ was used to ensure that the variation is independent from the magnitude of $\vec{u}_{n,m}$.

2.2 Numerical method

The system of parabolic nonlinear coupled equations given by Eq. (4) is solved numerically using finite differences. The partial differential equation is discretized implicitly using second order backward differencing in the streamwise direction, and fourth order central differencing in the normal direction. For the points neighboring the boundaries, second order central differencing in the normal direction was used. The resulting coupled algebraic equations form a block pentadiagonal system which is solved by LU decomposition.

At each step in the streamwise direction, the nonlinear terms are evaluated iteratively The iterative process is used to enforce both the normalization condition and the convergence of the nonlinear terms. In order to speed up the computation a A Gauss-Siedel iteration scheme with successive over-relaxation is used. The nonlinear products are evaluated in the time domain. The dependent variables in the frequency domain are converted to the time domain by an inverse Fast Fourier Transform subroutine. The nonlinear products are evaluated and the results are transformed back to the frequency domain.

The complex wavenumber is updated at each iteration and the variation in the shape function is monitored through Eq. (5). The iteration is considered converged when the normalization condition is no larger than a given small threshold.

3. SUBHARMONIC INSTABILITY

Kachanov and Levchenko (1984) identified a nonlinear secondary instability mode where a two-dimensional (2D) Tollmien-Schlichting (TS) wave excites a three-dimensional (3D) wave having half the frequency of the 2D wave. This 3D wave is stable according to linear stability theory. The observed growth is due to the nonlinear interaction with the 2D TS wave. Figure 1 shows the evolution of the 2D and 3D waves and compares the experimental results obtained by Kachanov and Levchenko with results obtained numerically using PSE. The figure also shows the decay of the 3D wave obtained with a linear analysis. The comparison between experimental and numerical results is good. The 2D

TS wave has frequency $f = 0.0496$ and the initial amplitude is $\epsilon = 0.00439$. The subharmonic 3D wave has half the frequency, spanwise wavenumber $\beta = 0.1333$ and initial amplitude $\epsilon_{(1,1)} = 0.000039$.

We are interested in determining whether this subharmonic resonance mechanism is predominant even when a third disturbance is present in the flow field. In order to perform this investigation, we seed the initial conditions for the experiment presented in Fig. 1 with a low amplitude 3D wave having the same frequency as the 2D wave and the same spanwise wavenumber as the 3D wave. This third disturbance is given by Fourier mode (2,1), which would be the mode arising from a fundamental secondary instability mode. The result is presented in Fig. 2. It shows that the Fourier mode (2,1) is not excited by the nonlinear interaction. Raising the initial amplitude of the 2D wave, mode (2,1) is excited. This is shown in figure 3. One sees that depending on the amplitude of the 2D wave, fundamental secondary instability mode is excited.

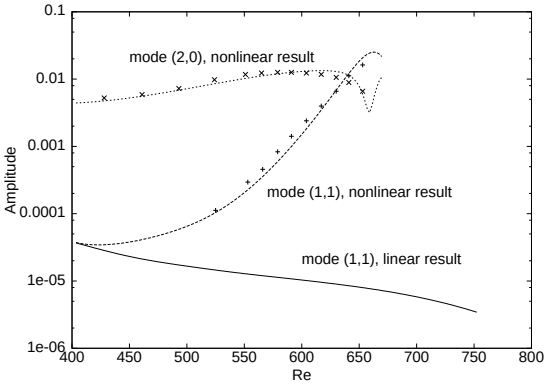

Figure 1: Comparison between experimental and numerical results for H-type secondary instability. Lines - PSE results, symbol - experimental results.

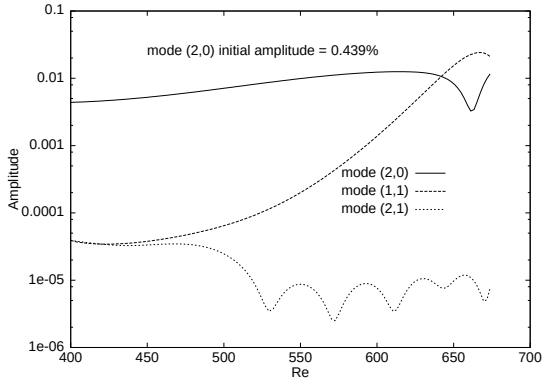

Figure 2: Numerical results for H-type instability including a fundamental oblique mode in the initial conditions.

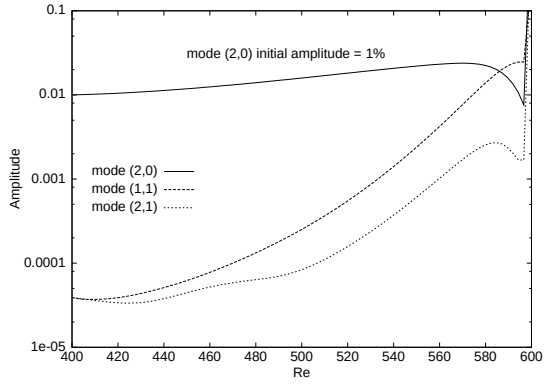

Figure 3: The same experiment presented in Fig. 2 with the initial amplitude of the 2D TS wave raised to 0.01.

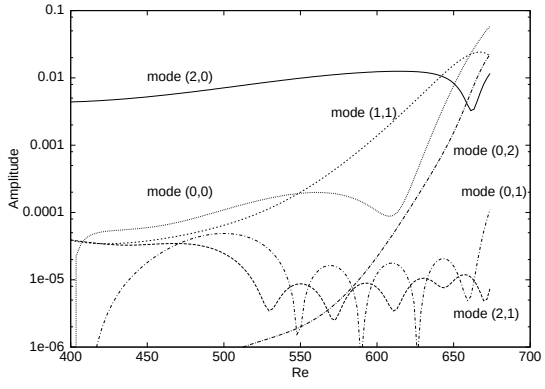

Figure 4: The same as in Fig. 2 showing the nonlinear development of stationary modes.

Figures 4 and 5 show the evolution of the mean flow distortion (MFD) given by the Fourier mode (0,0), and spanwise periodic longitudinal vortices, given by Fourier modes (0,1) and (0,2). The oblique TS modes are responsible for the growth of this longitudinal stationary modes. At the latter stages of the nonlinear development it is possible to

observe a very strong growth of the MFD and of mode (0,2). For the 2D TS initial amplitude of 0.00439, the longitudinal stationary mode (0,1) remains at a low amplitude, of the same order of magnitude as mode (2,1). For the second experiment, where the initial amplitude of the 2D TS wave was raised to 0.01, mode (0,1) is excited. The result suggests that the growth of mode (0,1) is due to the nonlinear growth of mode (2,1). The growth of mode (0,1) has a strong influence on the resulting spanwise periodicity responsible for the peak and valley regions.

A third numerical experiment was performed. In the two previous experiments the oblique waves were stable according to linear theory, and they where excited by the nonlinear interaction. Lowering the spanwise wavenumber of the oblique waves it is possible to investigate the behavior of the nonlinear interaction for linearly unstable oblique modes. Figure 6 shows an experiment for which the 2D TS wave is identical to the 2D wave of the previous experiments, but the wavenumber of the oblique waves was lowered to $\beta = 0.04$. For this spanwise wave number and for the given frequency, mode (2,1) is already unstable, while mode (1,1) did not cross the lower branch of the neutral curve yet. The growth of mode (2,1) is small, but as the disturbances travel downstream, its amplitude becomes greater than that of mode (1,1). The result shows that, depending on the growth rate of the oblique waves the characteristic feature of subharmonic secondary instability may change due to the stronger nonlinear excitation of a fundamental mode. In summary, whether a given laminar flow will undergo subharmonic or fundamental secondary instability depends on the initial amplitude of the modes and also on their growth rate.

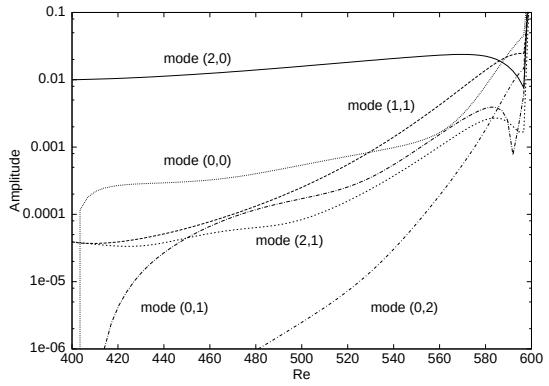

Figure 5: The same as in Fig. 4 with the initial amplitude of the 2D TS wave raised to 0.01.

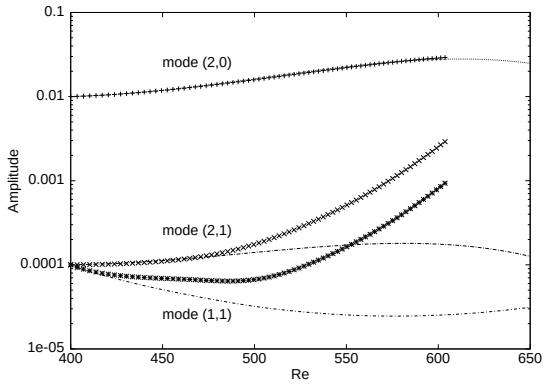

Figure 6: The same as in Fig. 3 with the oblique modes spanwise wavenumber lowered to 0.04.

The vorticity distribution for H-type secondary instability is presented in Fig. 7 and Fig. 8. In both figures the disturbances are followed up to a streamwise position where the computation presents convergency problems due to the growth of a large number of Fourier modes. That can be taken as an early sign of breakdown to turbulence. Figure 7 presentes de vorticity distribution for the experiment presented in Fig. 2 and Fig. 8 the vorticity distributin for the experiment presented in Fig. 3 In the experiment presented in Fig. 3 the subharmonic mode is still dominant despite the excitation of the fundamental mode (2,1). As a consequence, the characteristic staggered vorticity pattern is observed.

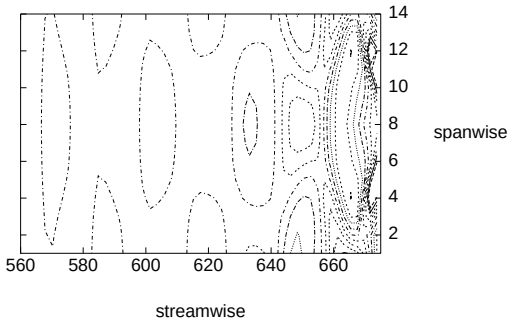

Figure 7: Distribution of vorticity in the ϕ, z plane for H-type instability.

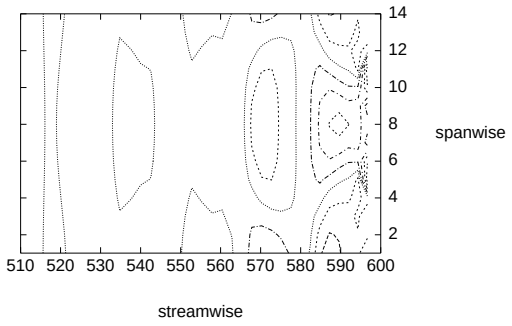

Figure 8: Distribution of vorticity in the ϕ, z plane for H-type instability seeded by an oblique fundamental mode.

4 FUNDAMENTAL INSTABILITY

The fundamental secondary instability mode was first identified by Klebanoff, Tidstrom and Sargent (1962). In this instability mode a two-dimensional wave excites an oblique wave of the same frequency. This oblique wave is stable according to linear stability theory as can be seen in the computations presented in figure 9. The figure also shows a comparison between PSE results and experimental results obtained by Cornelius (1985). The 2D TS wave has frequency $f = 0.01932$ and initial amplitude $\epsilon = 0.01$. The fundamental 3D wave has the same frequency, spanwise wavenumber $\beta = 0.264$ and initial amplitude $\epsilon_{(1,1)} = 0.0015$.

Figure 10 shows results of a similar experiment, which included a subharmonic oblique wave (with have the frequency of the 2D TS wave) in the initial condition. It shows that the subharmonic oblique wave is strongly destabilized by the 2D TS wave. By comparing this result with those for lower and higher initial 2D TS wave amplitude, presented in Fig. 11 and 12 it is observed that the destabilization of the fundamental mode is strongly dependent on the amplitude of the 2D TS wave. In order to have fundamental secondary

instability instead of subharmonic secondary instability it would be necessary to suppress subharmonic modes all together or to have a significantly strong initial 2D disturbance.

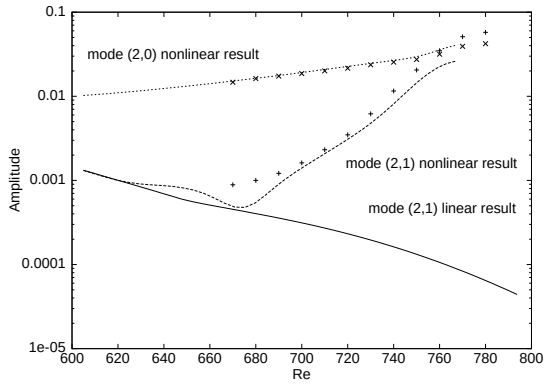

Figure 9: Comparison between experimental and numerical results for K-type secondary instability. Lines - PSE results, symbol - experimental results.

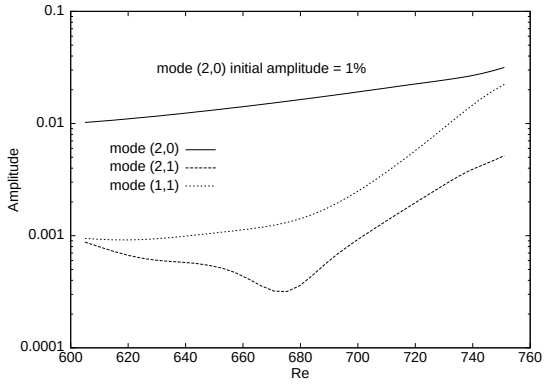

Figure 10: Numerical results for K-type secondary instability, including a subharmonic oblique mode in the initial conditions.

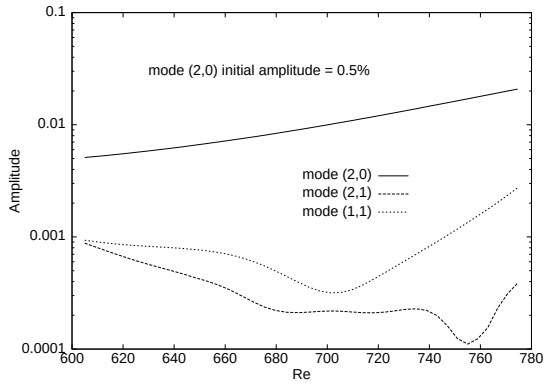

Figure 11: The same as in Fig. 10 with the initial amplitude of the 2D TS wave lowered to 0.005.

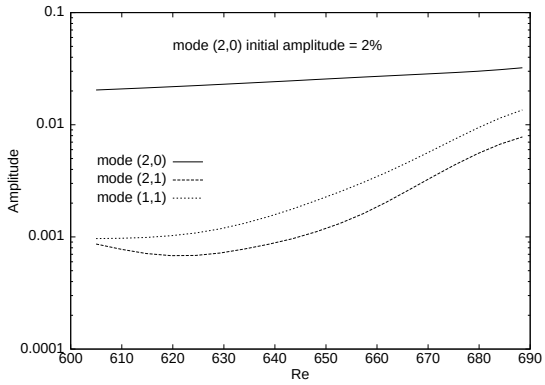

Figure 12: The same as in Fig. 10 with the initial amplitude of the 2D TS wave raised to 0.02.

On the other hand, lowering the wavenumber of the oblique disturbances it is possible to have a situation where the fundamental oblique mode (Fourier mode (2,1)) is already unstable, while the subharmonic oblique mode (Fourier mode (1,1)) has not crossed the lower branch of the neutral curve yet. In this case the relative amplitude of the 2D TS wave and of the fundamental oblique wave results in a strong destabilization of the last as seen in Fig. 13. Never the less, the subharmonic oblique mode continues to be strongly destabilized by the 2D TS wave. Figure 14 shows that the mean flow distortion and the longitudinal modes (0,1) and (0,2) are also amplified by the nonlinear interaction.

Based on the limited number of numerical experiments presented in this paper, it is possible to conclude that subharmonic secondary instability should be more easily observed. This is because the subharmonic oblique mode is strongly destabilized by the nonlinear interaction, even when the subharmonic mode has a lower growth rate than the fundamental oblique mode. To confirm this conclusion a larger number of experiments for different frequencies, spanwise wavenumbers and initial amplitudes would be necessary.

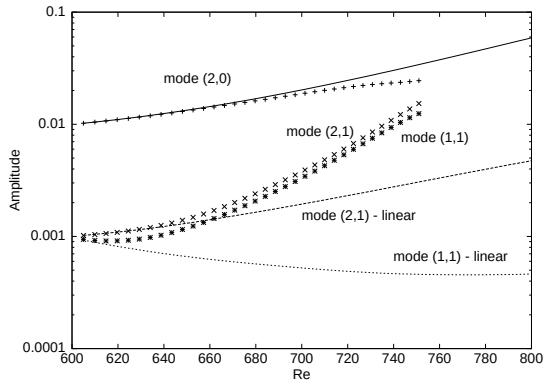

Figure 13: The same as in Fig. 10 with the oblique modes spanwise wavenumber lowered to 0.06.

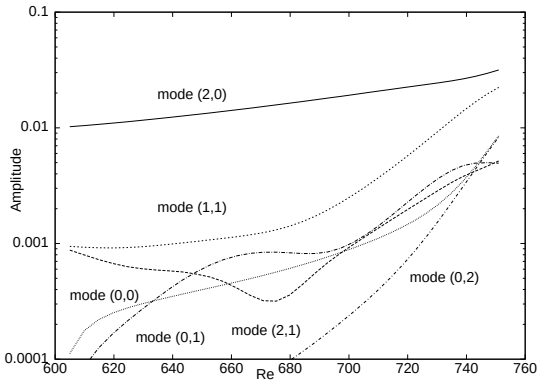

Figure 14: The same as in Fig. 10 showing the nonlinear development of the mean flow distortion and of longitudinal vortices.

The vorticity distribution for K-type secondary instability is presented in Fig. 15 and 16. Figure 15 corresponds to the experiment presented in Fig. 9 and Fig. 16 to the experiment in Fig. 10. The major aligned patter is still dominant, but it is possible to observe the growth of small cells of staggered pattern at about $Re = 739$.

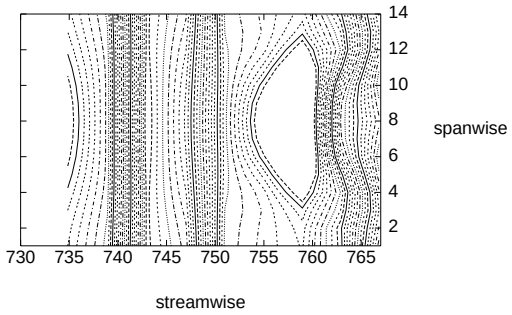

Figure 15: Distribution of vorticity in the ϕ, z plane for K-type secondary instability.

5. CONCLUSIONS

In the present paper numerical simulations have been presented in order to investigate the characteristics of K-type and H-type secondary instabilities. The results show that the excitation of fundamental modes depend strongly on the initial amplitude of the 2D TS wave. Growing subharmonic and fundamental oblique modes were also investigated. The results show that, since the fundamental mode has higher frequency it becomes unstable earlier than the subharmonic mode resulting in fundamental secondary instability. The subharmonic mode has a very strong nonlinear growth. As a result, the characteristic subharmonic staggered pattern for the vorticity distribution can be observed in results where both modes are included. In natural conditions it is likely that subharmonic instability will be more easily observed.

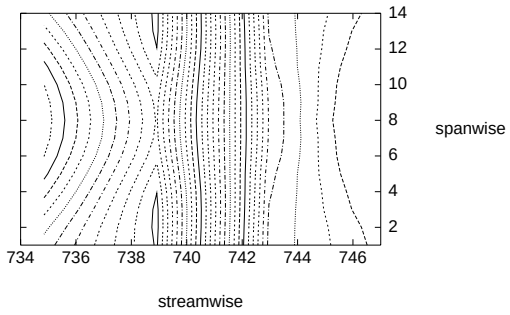

Figure 16: Distribution of vorticity in the ϕ, z plane for K-type secondary instability seeded by an oblique subharmonic mode.

5. ACKNOWLEDGMENT

The first author would like to acknowledge the financial support received from FAPESP (Fundação de Amparo à Pesquisa dos Estado de São Paulo) for the participation in the ENCIT 2000.

REFERENCES

Cornelius, K. C. 1985. *Three-Dimensional Wave Development During Boundary Layer Transition.* Tech. rept. LG85rr0004. Lockheed Corp.

Herbert, Th. 1988. Secondary Instability of Boundary Layers. *Annu. Rev. Fluid Mechanics*, **20**, 487–526.

Kachanov, Y. K., and Levchenko, V. Y. 1984. The Resonant Interaction of Disturbances at Laminar-Turbulent Transition in a Boundary Layer. *J. Fluid Mechanics*, **138**, 209–247.

Klebanoff, Y. S., Tidstrom, K. D., and Sargent, L. M. 1962. The Three-Dimensional Nature of Boundary Layer Stability. *J. Fluid Mechanics*, **12**, 1–34.

Mendonça, M. T. 1997. *Numerical Analysis of Görtler Vortices /Tollmien-Schlichting Waves Interaction With a Spatial Nonparallel Model.* Ph.D. thesis, The Pennsylvania State University.

Mendonça, M. T., Pauley, L. L., and Morris, P. J. 2000a. Influence of Wave Frequency on Görtler Vortices, Three-dimensional Tollmien-Schlichting Waves Interaction. *Revista Brasileira de Ciências Mecânicas - RBCM*, **XXII**.

Mendonça, M. T., Morris, P. J., and Pauley, L. L. 2000b. Interaction Between Görtler Vortices and two-dimensional Tollmien-Schlichting waves. *Physics of Fluids*, **12**(5), 1–11.